Title

The Role of Ubiquitin-like Modifier FAT10 in Adipose Metabolism

Author

Tran, Peter Huy

Publication Date

2024

Peer reviewed|Thesis/dissertation

UNIVERSITY OF CALIFORNIA

Los Angeles

The Role of Ubiquitin-like Modifier FAT10 in Adipose Metabolism

A thesis submitted in partial satisfaction of the requirements for the degree Master of Science

in Physiological Science

by

Peter Huy Tran

2024

ABSTRACT OF THE THESIS

The Role of Ubiquitin-like Modifier FAT10 in Adipose Metabolism

by

Peter Huy Tran

Master of Science in Physiological Science

University of California. Los Angeles, 2024

Professor Claudio Javier Villanueva, Co-Chair

Professor Andrea Hevener, Co-Chair

In the United States, approximately a third of the population is affected by obesity, with exercise and dietary modifications implemented as the traditional methods of combatting metabolic-related diseases. We identified ubiquitin-like modifier FAT10 as a novel protein significantly correlated with adiposity. Despite the scientific literature describing FAT10 in various inflammation-driven disorders and types of cancers, the mechanism by which FAT10 regulates metabolic pathways in white and brown adipose tissue is not well understood. Here, we demonstrate the dynamic expression of FAT10 in adipose tissue and show adipose-specific FAT10 gain-of-expression mice mitigates weight gain by altering lipid metabolism and energy homeostasis. Within white adipose depots, small adipocytes present in significantly higher numbers with FAT10 overexpression compared to controls, while brown adipose depots present with a decrease in lipid content. Adipose tissue overexpression of FAT10 induces lipolysis and fuels catabolic processes such as fatty acid oxidation and UCP1-dependent non-shivering thermogenesis. Our findings indicate FAT10 plays a diverse and critical role in both white and

brown adipose tissue regarding the regulation of lipolysis, fatty acid oxidation, and UCP1-dependent thermogenesis, suggesting a potential therapeutic target to combat obesity and metabolic-associated diseases.

The thesis of Peter Huy Tran is approved.

Zhenqi Zhou

Xia Yang

Stephanie Correa Van Veen

Claudio Javier Villanueva, Co-Chair

Andrea Hevener, Co-Chair

University of California, Los Angeles

2024

TABLE OF CONTENTS

LIST OF FIGURES AND TABLES

ACKNOWLEDGEMENTS

I want to express my heartfelt thanks to my family and friends for their unconditional support throughout my academic journey. Special thanks to Timothy M. Moore, Alice M. Ma, Holly J. Do, Arnav Singh, Annemarie E. Lawrence, Emma Y. Yim, Hirotaka Iwasaki, Alexander R. Strumwasser, and Jonathan Wanagat for their contributions to my thesis. Thank you to my committee members and research mentors, Dr. Andrea Hevener and Dr. Zhenqi Zhou, for their invaluable guidance and support.

Introduction

Ubiquitin D (UBD) or human leukocyte antigen-F adjacent transcript 10 (FAT10) is a ubiquitin-like modifier (UBL) that directly targets proteins for proteasomal degradation. Ubiquitination as a post-translational modification process regulates a myriad of physiological functions exclusively in mammalian species[1]. Similar to other unique derivations of ubiquitination processes like SUMOylation and NEDDylation, FAT10 participates in a ubiquitin-independent process called FAT10ylation[7]. FAT10ylation is catalyzed by activating E1 enzyme UBA6 and conjugating E2 enzyme UBA6-specific enzyme to initiate FAT10 ligation to an E3 enzyme[7,12]. Interestingly, unlike in canonical ubiquitination processes where ubiquitin is removed from its substrate protein, FAT10 remains attached and is collectively degraded through the 26S proteasome[12]. FAT10 has varying basal levels of expression across diverse tissues but remains highly expressed in cells of the immune system as interferon gamma (INF-y) and tumor necrosis factor alpha (TNF-α) regulate its induction[7,12]. With FAT10 closely associated with various inflammation-driven pathways and its regulatory function as a UBL, many studies have focused on how FAT10 may have a critical role in the pathogenesis of several cancers and immune-driven diseases[6,8,11,12,14].

Recent studies have shown how perturbations to FAT10 expression across the body and in specific tissues may also influence various metabolic processes. Global knockout of FAT10 in mice has been shown to have reduced adiposity and protective benefits from age-associated obesity. This metabolic reprogramming due to the loss of ubiquitous FAT10 suggests its influence on immune-metabolic-related pathways surrounding adipose metabolism[3]. However, adipose-specific studies looking at the role of FAT10 in white and brown adipose tissue metabolism remain inadequately understood. Numerous studies have also shown uncoupling

protein 1 (UCP1)-dependent thermogenesis may impact adiposity. UCP1 is primarily found in multilocular brown adipose tissue, along with some thermogenic function in beige adipose tissue, a hybrid between brown and white adipose[16]. Through UCP1-mediated proton gradient dissipation along the inner mitochondrial membrane, energy is lost as heat, contributing to non-shivering thermogenesis[15,16]. How FAT10 may regulate either UCP1-dependent non-shivering thermogenesis in brown adipose tissue and its downstream effects on adiposity is poorly understood.

Here, we sought to determine how adipose-specific gain-of-expression of FAT10 may regulate adiposity and downstream metabolic processes in white and brown adipose tissue. To address this, we constructed an adeno-associated virus (AAV) with an adiponectin promoter and generated various mouse models to look at the local morphological and whole-body metabolic adaptation as a result of the tissue-specific overexpression. Our studies determined that adipose-specific FAT10 overexpression significantly reduces adiposity through the breakdown of triglycerides which later fuel catabolic processes that significantly alter energy homeostasis. These observations identify how FAT10 regulates lipid metabolism in white and brown adipose and may potentially be used as a therapeutic to modulate adiposity and combat adipose-driven metabolic syndrome.

Materials and Methods

Primer List for qPCR

Species	**Gene Symbol**	**Forward**	**Reverse**
Mouse	18S	CGCCGCTAGAGGTGAAATTCT	CGAACCTCCGACTTTCGTTCT
	Abca1	CTTCCCACATTTTTGCCTGG	AAGGTTCCGTCCTACCAAGTCC
	Abhd5	AGTGATGCGGAAGAAGTGGA	TAGGGCCCTGATCCAAACTG
	Acad1	TGCACACATACAGACGGTGC	CATGGAAGCAGAACCGGAGT
	Acadm	GCAGCCAATGATGTGTGCTTAC	CACCCTTCTTCTCTGCTTTGGT
	Acox1	GCCCAACTGTGACTTCCAT	GGCATGTAACCCGTAGCACT
	Acsl1	ACCATCAGTGGTACCCGCTA	CTTCCAACCAACACCCTCAT
	Atgl	CAACGCCACTCACATCTACG	ACCAGGTTGAAGGAGGGATG
	CD36	GTGCAAAACCCAGATGACGT	TCCAACAGACAGTGAAGGCT
	Cidea	TCTGCAATCCCATGAATGTC	GTGGCTGATAGGGCAGTGAT
	Elov3l	CCAACAACGATGAGCAACAG	CGGGTTAAAAATGGACCTGA
	Fabp4	TTCGATGAAATCACCGCAGA	GGTCGACTTTCCATCCCACTT
	Hsl	TGAGATTGAGGTGCTGTCGT	GTACCTTGCTGTCCTGTCCT
	Lpl	AGGACCCCTGAAGACAC	GGCACCCTCAACTCTATA
	Mgl	GCTTCCGACGGAC	TGAATAACCGTTG

		TTACAAC	GGATGCT
	UBD (1)	CCTTACCCTGAAG GTGGTGA	CTTCCAGCTTCTTT CCGTTG
	UBD (2)	CCTTACCCTGAAG GTGGTGA	CTTCCAGCTTCTC GTTG
	UCP1	GGAAAGGGACGA CCCCTAATC	CCGGCAACAAGA GCTGACA

Antibody List

REAGENT/ANTIBODY	SOURCE	CATALOG #
UBD	ThermoFisher (Invitrogen)	MAS-32487
HSP90	Cell Signaling	4877S
GAPDH	Cell Signaling	5174S
p-HSL	Cell Signaling	4139T
HSL	Cell Signaling	4107T
ATGL	Cell Signaling	2138S
UCP1	Cell Signaling	14670S

Human Subjects

Gene-Derived Correlations Across Tissues (GDCAT)

A cohort of 310 human subjects (between the ages of 20-79) from the UCI Systems Genetics Lab web interface Gene-Derived Correlations Across Tissues (GDCAT) (n=210 male and n=100 female) underwent correlative analysis that is used to help identify mechanisms of organ crosstalk between various tissues[23]. FAT10 analyses were compared between both males and females in visceral white adipose tissue as the originating tissue.

METSIM studies

Genetic association and gene expression analyses were conducted on data collected from the metabolic syndrome in men (METSIM) study[24]. The study consists of a cohort of 10,197 men (between the ages of 45 and 73) randomly selected from Kuopio, Eastern Finland, between 2005 and 2010. For this study, no additional human samples were acquired. Correlative analysis was conducted between adipose FAT10 expression and self-reported questionnaire responses related to exercise frequency.

Animals

UCLA Exercise Hybrid Mouse Diversity Panel (eHMDP)

All mice were obtained from The Jackson Laboratory and bred at University of California, Los Angeles. Mice were maintained on a chow diet (Ralston Purina Company) until 12 weeks of age when they either were kept in normal husbandry cages or housed with an in-cage running wheel. Exercise trained mice (TRN) housed with the running wheel were then allowed to exercise voluntarily for 30 days. Prior to tissue harvesting, running wheels were locked to allow for 24-

hour acute training recovery and euthanized the following day. Additionally, this resource was established to provide a platform for high-resolution genome-wide mapping and systems-level analysis of gene-gene and gene-trait relationships. Animal studies were approved by the University of California, Los Angeles Institutional Animal Care and Use Committee.

Acute Running Treadmills

Mice were trained on the Columbus Exer 3/6 Treadmill for 60 minutes, starting at 5 meters/minute (m/min) at a 5-degree incline for 15 minutes. The speed was then increased by 1 m/min until 15 m/min. Post-exercise recovery times were then determine based on the experimental design. All animals were monitored during the 60-minute acute training session.

Animal characteristics

Blood and tissues were taken from 6–8-month-old, 6 hour fasted mice. Circulating parameters were analyzed: glucose (Hemocue America 110723), insulin and leptin (Meso Scale Discovery K15124C-1), and non-esterified fatty acids (Fujifilm 27676491, 99934691, 99534791, 99134891, 99335191). Intraperitoneal insulin tolerance tests (IPITT, 0.7 U/kg) were performed with 6 or 16 hours fasting. Exercise performance and training (30d of volitional in cage wheel running) as previously described[18]. Body fat and lean fat were determined by NMR (Bruker). Oxygen consumption, carbon dioxide production, respiratory exchange ratio, and energy expenditure were determined using the Promethion metabolic screening system (Sable Systems). Body temperature measurements were conducted using an implantable RFID microchip (BMDS IMI-1000 Transponder) inserted subcutaneously while animals were under anesthesia. Body temperature measurements were taken using a wireless reader (BMDS DAS-8006 IUS).

Adeno-associated virus (AAV) Injection (Local gWAT Injection)

Male C57BL/6J wild-type mice (8 months) (The Jackson Laboratory, #000664) were anesthetized with isoflurane and fixed into a supine position. The midventral line region was shaved and cleaned with ethanol. A 1.5–2 cm midline incision was made in the skin followed by separation of the underlying musculature to expose the gonadal white adipose tissue (gWAT). 1×10^{11} GC/μl of AAV8-hAdp-mUBD (AAV-FAT10) (Vector Biolabs, AAV-275456) dissolved in 50 uL of saline was injected directly into the left gWAT. The same amount of control virus (AAV-Control) and saline volume was injected into the other side of gWAT. The body wall was sutured, and the wound was closed with wound clips with animals recovered on a heating pad. To prevent infection, antibiotic ointment containing polymyxin B sulfate, bacitracin zinc, and neomycin was applied to the closed wound. Animals were observed daily for any signs of inflammation. 7 days after surgery, the wound clips were removed. After four weeks of AAV injection, mice were euthanized by isoflurane overdose followed by cervical dislocation.

Adeno-associated virus (AAV) Injection (Tail Vein Injection)

Male C57BL/6J wild-type mice (6 months) (The Jackson Laboratory, #000664) were restrained in an injection cone one at a time, exposing the lateral tail vein. The lateral tail vein is sterilized and pre-warmed to vasodilate the exposed vessel. Either 1×10^{11} GC/μl of AAV8-hAdp-mUBD (AAV-FAT10) (Vector Biolabs, AAV-275456) dissolved in 50 uL of saline or control virus was injected directly into the lateral tail vein. Animals were then observed daily for any abnormalities. After eight weeks of AAV injection, mice were euthanized by isoflurane overdose followed by cervical dislocation.

Adeno-associated virus (AAV) Injection (Local BAT Injection)

Male C57BL/6J wild-type mice (8 months old) (The Jackson Laboratory, #000664) were anesthetized with isoflurane and fixed into a supine position. The fur on the subscapular region was shaved where either 1×10^{11} GC/μl of AAV8-hAdp-mUBD (AAV-FAT10) (Vector Biolabs AAV-275456) dissolved in 50 uL of saline or control virus was injected. Animals were then observed daily for any abnormalities. After eight weeks of AAV injection, mice were euthanized by isoflurane overdose followed by cervical dislocation.

Cell culture and treatments

Cell lines, 3T3-L1 fibroblasts, were maintained in high glucose DMEM, 10% fetal bovine serum with penicillin/streptomycin. To obtain differentiated white adipocytes, cells were allowed to reach confluence and switched the media to high glucose DMEM, 10% fetal bovine serum, dexamethasone (1uM), IBMX (0.5 mM), insulin (5ug/mL) with penicillin/streptomycin for 2 days. Media is then switched to DMEM, 10% fetal bovine serum, and insulin (5ug/mL) with penicillin/streptomycin for an additional 2 days. Lastly, media is switched to high glucose DMEM, 10% fetal bovine serum with penicillin/streptomycin for the remaining four days.

Immunoblot and densitometry analysis

Mouse tissue samples were pulverized in liquid nitrogen and homogenized in RIPA lysis buffer containing freshly added protease (complete EDTA-Free, Roche) and phosphatase inhibitors (Phosphatase Inhibitor Cocktail 2, Sigma). All lysates were clarified, centrifuged, and resolved by SDS-PAGE. Samples were transferred to PVDF membranes and subsequently probed with

the following antibodies for protein listed in antibody list. Densitometric analysis was performed using BioRad Quantity One image software.

DNA & RNA extraction, cDNA synthesis, quantitative RT-PCR

DNA and RNA were extracted from a homogenous portion of gonadal white adipose and brown adipose tissue homogenate using DNeasy/RNeasy Isolation kits (Qiagen) as described by the manufacturer. Isolated DNA and RNA was tested for concentration and purity using a NanoDrop Spectrophotometer (ThermoScientific). Isolated RNA was converted into cDNA, checked for purity, and qPCR of the resulting cDNA levels was performed using the Applied Biosystems Quantstudio 5. All genes were normalized to the housekeeping gene 18S.

ImageJ Adipocyte Quantification

Analysis of adipocyte cell area and count were processed through ImageJ open-source automated software *Adiposoft*[21]. For further descriptions and instructions about *Adiposoft*, please visit https://imagej.net/plugins/adiposoft. Quantification and statistical analyses on adipocytes were conducted on Python. All analyses are open-source and available on the following GitHub link: https://github.com/peterxtran/UCLA-FAT10-Thesis. For any questions, please contact the first- or corresponding author.

Statistical analysis

Values presented are expressed as means ± SEM. Statistical analyses were performed using Student's t-test when comparing two groups of samples or one-way analysis of variance (ANOVA) with Tukey's post hoc comparison for identification of significance within and

between groups using GraphPad Prism 10 (GraphPad Software). Mean differences between groups over time were assessed by repeated measures analysis of variance. Significance was set a priori at $P < 0.05$.

Results

Dynamic FAT10 Expression in Adipose Tissue

Human leukocyte antigen (HLA)-F adjacent transcript 10 (FAT10), also known as ubiquitin D (UBD), is a ubiquitin-like modifier found within the human MHC locus[5]. Early studies first characterized the role of FAT10 in immune function due to its high inducibility to pro-inflammatory cytokines such as interferon gamma (IFNy) and tumor necrosis factor (TNF)[5,6]. While FAT10 has been extensively studied in various immune-related systems, recent studies have begun to expand on the role of FAT10 in other pathologies such as osteosarcoma[2], metabolic-associated fatty liver disease[4], and adiposity[3]. However, as the role of FAT10 has been described uniquely in these different diagnoses, it remains unclear the downstream pathways affected by fluctuating FAT10 expression levels. FAT10 has been shown to serve as either an early biomarker for advanced disease prognosis[8] or have regulatory protective function[9]. With recent studies unraveling the complex role of FAT10 in diverse tissue types, we interrogated transcriptomic data from the Gene-Derived Correlations Across Tissues (GDCAT)[19,20,23]. We saw the vast FAT10 expression in various tissues but found a high number of transcripts significantly correlated with FAT10 primarily in visceral white adipose tissue (Figure 1A). While there continues to be a strong correlation between FAT10 expression and immune-regulated pathways, the role of this ubiquitin-like modifier in top tissue origins such as white adipose tissue is poorly understood.

To first contextualize the expression of FAT10 in adipose tissue, we did a comparative screen of FAT10 gene expression across various tissues in male and female C57BL/6J mice (Figure 1B). Across the comparative screen, FAT10 gene expression was highest in the spleen, an immune-rich tissue system. Surprisingly, visceral gonadal white adipose tissue (gWAT) also

expresses high levels of FAT10, suggesting its critical role in regulating and modulating adipose-specific signaling pathways.

With previous studies showing how a global knockout of FAT10 significantly reduces adiposity[3], we explored whether chronic exercise in mice, known to decrease adiposity, would affect FAT10. Through the exercise Hybrid Mouse Diversity Panel (eHMDP), we looked to see if 30 days of voluntary chronic exercise with an in-cage running wheel had any impact on adipose FAT10 gene expression. FAT10 was the only differentially expressed gene significantly correlated with adiposity between sedentary (SED) and chronic exercise-trained (cTRN) mice. Further studies showed that cTRN mice exhibited a decrease in whole-body adiposity, correlating with an increase in total running distance and a reduction in adipose FAT10 gene expression (Figure 1C). Similar correlative relationships were seen in the Metabolic Syndrome In Men (METSIM) study, which utilized samples collected from over 10,000 Finnish men to investigate both the genetic and non-genetic risk factors associated with type 2 diabetes, cardiovascular disease (CVD), and other metabolic diseases. Finnish men who reported recommended exercise levels exhibited lower adipose FAT10 expression levels compared to those who reported little to no exercise[17] (Figure 1D). Since FAT10 is highly inducible to inflammatory signals, we sought whether different recovery times post-exercise cessation would influence FAT10 expression in adipose tissue[27].

To test the effect of post-exercise recovery on gWAT FAT10 expression, mice were subjected to 60 minutes of acute exercise on a rodent treadmill and were sacrificed at 0-hour, 12-hour, and 24-hour post-exercise cessation. Immunoblots and densitometric analyses were then performed to examine FAT10 protein expression in gWAT between acute exercise-trained (aTRN) and SED mice (Figure 1E). Immediately following acute exercise with no recovery,

FAT10 protein expression significantly increased approximately four-fold and remains elevated 12 hours post-exercise cessation. 24 hours of recovery after acute training, FAT10 protein expression between aTRN and SED mice is normalized. In addition to elucidating the role of exercise in regulating adiposity and the expression of the adipose FAT10 gene and protein, our findings underscore the significance of various post-exercise recovery periods in shaping the dynamic profile of FAT10. By delineating the unique relationship between FAT10 and adiposity, it is crucial to delve into tissue-specific investigations to improve our understanding of its role within adipose tissue.

FAT10 Overexpression Changes White Adipocyte Morphology

With respective changes between adiposity and adipose FAT10 expression, we hope to characterize further how FAT10 specifically influences adipocyte form and function. Using an AAV8-Adiponectin-FAT10 (AAV-FAT10), we hypothesized that the local overexpression of FAT10 in the gWAT would exhibit significantly different histological phenotypes. We aestheticized 6-month-old C57BL/6J males and made a 1.5–2 cm midline incision in the lower abdominal region, exposing the bilateral gWAT. One gWAT depot was injected with the AAV-FAT10 (local-AAV-FAT10), while the other gWAT depot was injected with an empty AAV vector (local-AAV-Control) (Figure 2A).

To confirm that the local-AAV-FAT10 had an overexpression of FAT10, we used reverse transcription-quantitative polymerase chain reaction (RT-qPCR) and conducted a pairwise statistical analysis (Figure 2B). The gWAT samples were then formalin-fixed and sectioned for hematoxylin and eosin (HE) staining which show significant differences in the density of adipocytes present (Figure 2C). Through the ImageJ *Adiposoft*[21], an automated open-source

software developed to analyze adipose tissue histology, histological HE sections were quantified for adipocyte count and cell area. Upon image quantification, a pairwise statistical comparison showed a significant increase in the number of small adipocytes in the local-AAV-FAT10 gWAT compared to the local-AAV-Control (Figure 2D). However, implications on the metabolic mechanism behind this difference in adipocyte distribution still need to be better understood. Whether this adipose hyperplasia phenotype is due to an increase in metabolic activity resulting in the decrease in lipid storage or disruption of homeostatic adipocyte function leading to lipodystrophy requires further investigation of how overexpression of FAT10 in adipose affects whole-body physiology.

Adipose-specific FAT10 Overexpression Affects Energy Homeostasis and Metabolism

To investigate the whole-body effects of adipose-specific overexpression of FAT10, male C57BL/6J mice were administered the same AAV-FAT10 or AAV-Control via the lateral tail vein (Figure 3A). For the following eight weeks, body weight and body composition, including lean muscle and fat mass, were measured. After approximately four weeks post-injection, AAV-FAT10 mice exhibited mitigated weight gained compared to AAV-Control mice (Figure 3B). AAV-FAT10 mice also showed a significant decrease in fat mass and an increase in lean mass (Figure 3C). There was no change in accumulated food or water intake (Supplemental Figure 1A). With a significant difference in body weight between the two cohorts, an intraperitoneal insulin tolerance test (ITT) was performed with either an overnight or six-hour fast. However, both ITTs showed no significant difference suggesting FAT10 overexpression does not affect insulin sensitivity (Supplemental Figure 1B, C). After a week of recovery, AAV-FAT10 and AAV-Control mice were housed in metabolic chambers for one week to measure energy

homeostasis. The respiratory exchange rate (RER), volume of oxygen consumed (VO2), and volume of carbon dioxide produced (VCO2) was significantly elevated in AAV-FAT10 mice (Figure 3D, E). Surprisingly, when normalized to body weight, AAV-FAT10 mice have significantly higher energy expenditure compared to control mice (Figure 3F). There was no significant change in locomotor activity (Supplemental Figure 1D). These findings show that adipose-specific FAT10 overexpression plays an underlying role in regulating adipose metabolism and energy homeostasis.

FAT10 Regulates Lipids Metabolism Through Lipolysis and Fatty Acid Oxidation

The changes in energy homeostasis in AAV-FAT10 mice are indications of downstream alterations in canonical molecular metabolic pathways[22]. While maintaining an overexpression of FAT10 of approximately two to three-fold of physiological range, we saw similar histological differences as seen with the local-AAV-FAT10 cohort (Figure 4A, Supplemental Figure 2A). Within the gWAT of AAV-FAT10 mice, adipocytes within the depot were significantly smaller compared to controls. Similarly, Oil Red O was performed on differentiated 3T3-L1 FAT10 overexpression cells, showing an overall decrease in triglycerides and lipids with increased FAT10 expression (Figure 4B, C). Understanding that adipose triglycerides are broken down into fatty acids to fuel catabolic processes, we also saw that there was a significant decrease in non-esterified fatty acids (NEFA) in the plasma and liver triglycerides (TG) in AAV-FAT10 mice (Supplemental Figure 2B, C).

To examine the impact of adipose FAT10 expression on downstream lipid pathways, gene expression analysis was conducted on differentiated 3T3-L1 FAT10 overexpression cells and white adipose tissue from AAV-FAT10 mice. Interestingly, pathways such as fatty acid

oxidation and lipolysis was trending upwards in AAV-FAT10 mice and significantly increased in 3T3-L1 FAT10 overexpression cells (Figure 4D, E). Together, our findings show how overexpression of FAT10 plays a role in regulating the breakdown of triglycerides through lipolysis to fuel catabolic pathways such as mitochondrial fatty acid oxidation.

FAT10 Regulates UCP1-Dependent Thermogenesis

With an increased in energy expenditure associated with upregulated FAT10, we investigated changes in brown adipose tissue (BAT) metabolism. BAT histology presented with a decreased in lipid droplets in AAV-FAT10 mice compared to controls (Figure 5A). With a decrease in lipid accumulation in the adipose depot, lipid metabolism pathways such as lipolysis and fatty acid oxidation were trending upwards similar to that seen in WAT (Figure 5B). To determine changes in thermogenic pathways, we also did gene and protein analysis of UCP1, a key mitochondrial protein involved in regulating non-shivering thermogenesis. While gene expression remained unchanged for UCP1, other thermogenesis genes had a trending increased (Figure 5C). Moreover, UCP1 protein levels were significantly increased, paralleling the increased in energy expenditure seen previously (Figure 5D). To further interrogate if FAT10 overexpression in brown adipose tissue translated to increased thermogenic capabilities, AAV-FAT10 was locally injected into the BAT (BAT-AAV-FAT10), where mice were fed a high-fat diet. Across seven weeks on high-fat diet, there was no change in body weight (Figure 5E). Body temperature remained unchanged under baseline room temperature conditions (Figure 5F). However, when placed in a four-degree cold-stress environment, BAT-AAV-FAT10 mice could maintain their core body temperature up to four hours, where the body temperature of the

controls gradually decreased over time (Figure 5F). Together, our findings show how overexpression of FAT10 can mediate UCP1-dependent thermogenesis.

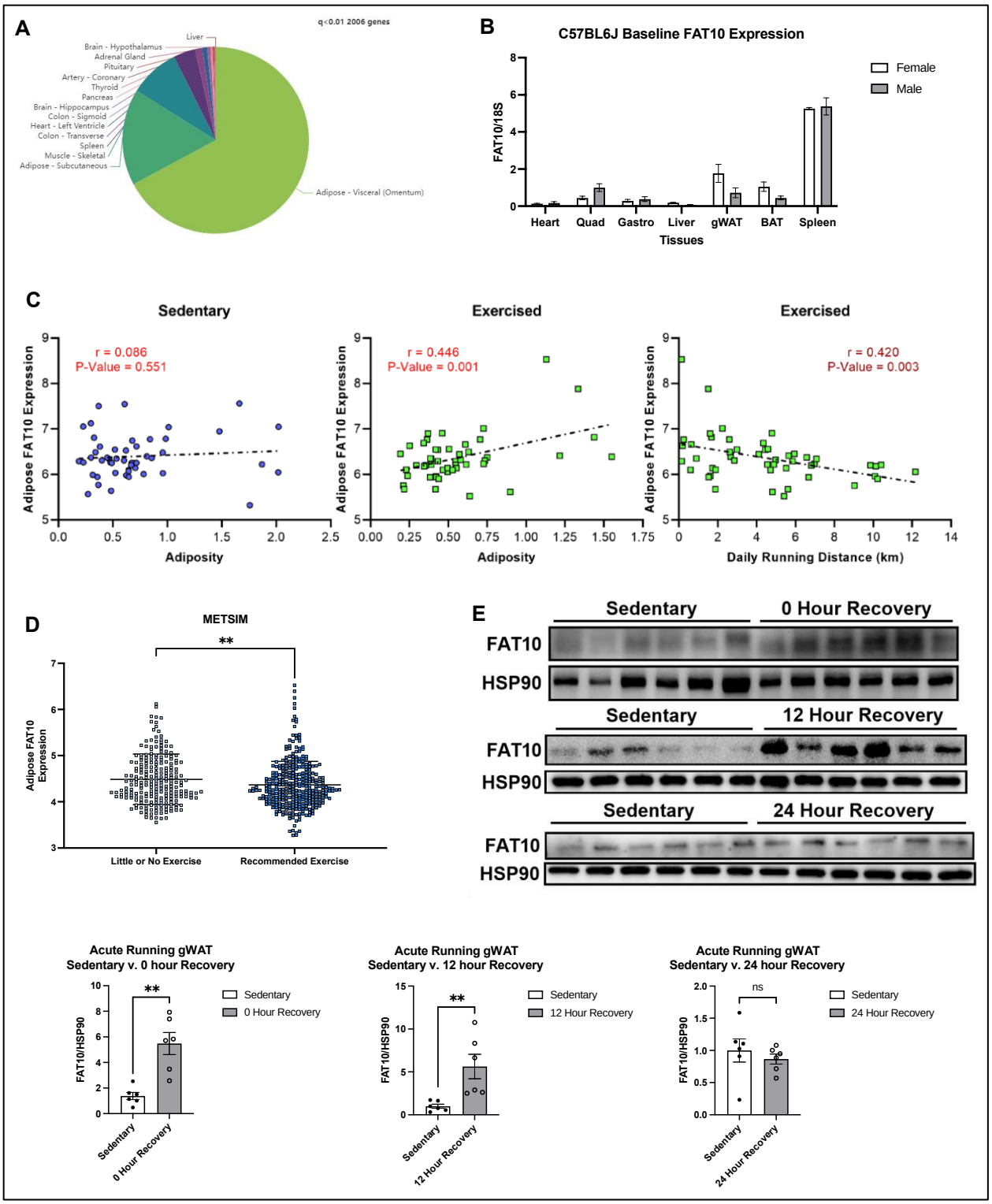

Figure 1. Dynamic FAT10 expression in adipose tissue. (A) Significantly correlated genes associated with FAT10 originating from visceral white adipose tissue. (B) Baseline FAT10 gene

expression in male and female C57BL/6J mice across diverse tissues. (C) White adipose FAT10 gene expression correlated with sedentary and exercise-trained mice adiposity of the eHMDP. Decreased adiposity is significantly correlated with decreased adipose FAT10 gene expression. (D) Adipose FAT10 gene expression amongst male human subjects who self-reported little to no exercise or performed the recommended amount of exercise. Exercise is significantly correlated with decreased adipose FAT10 gene expression. (E) Immunoblot and densitometric analysis of FAT10 protein expression in gonadal white adipose tissue (gWAT) was conducted on acute exercise male mice following different post-exercise recovery timepoints. FAT10 protein expression increases post-exercise following no recovery and remains elevated until 12-hours post-exercise recovery. Following 24-hours post-exercise recovery, FAT10 protein levels are normalized. Data are presented as mean ± SEM. * $p < 0.05$, ** $p < 0.005$.

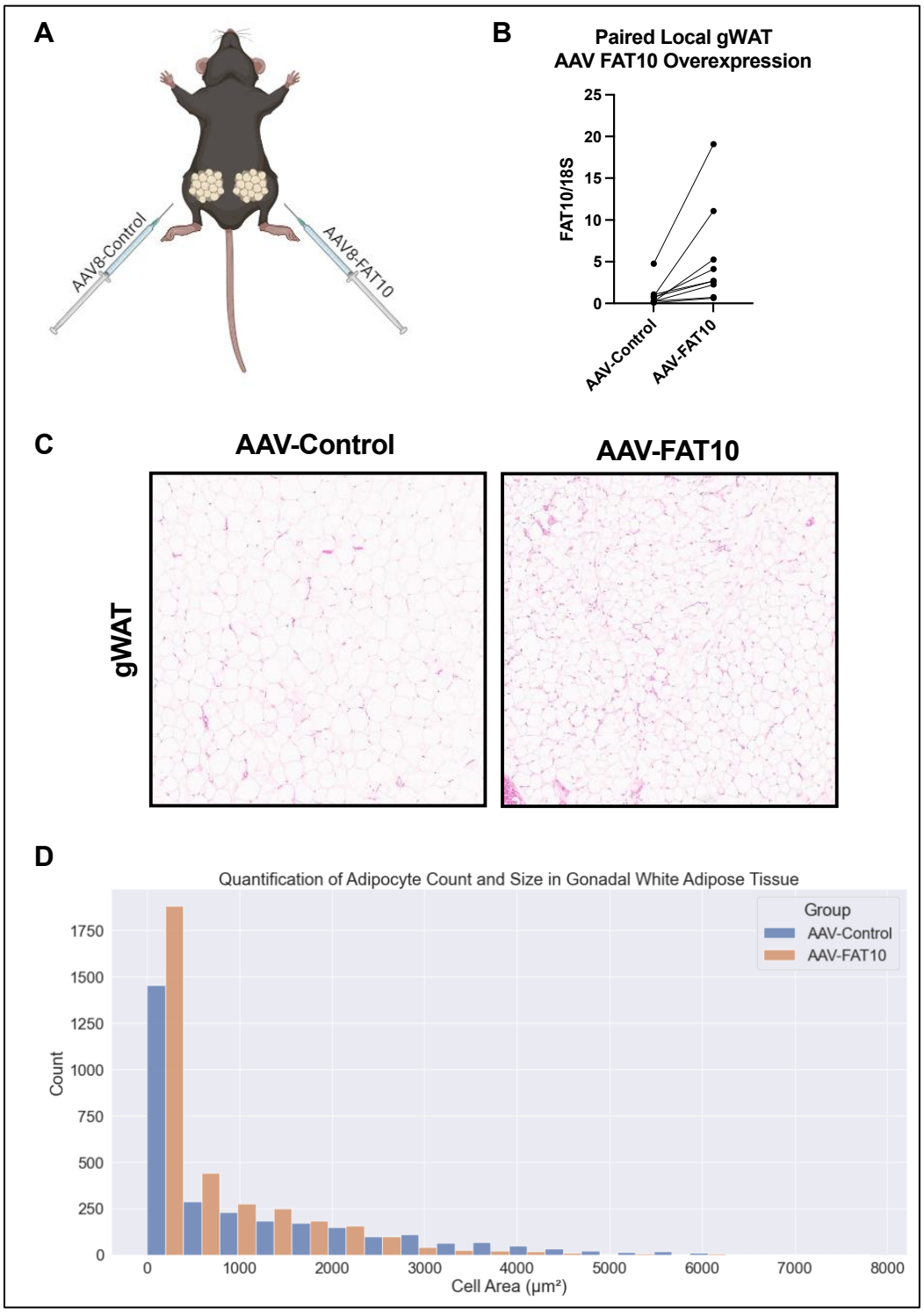

Figure 2. FAT10 overexpression changes white adipocyte morphology. (A) Schematic depicting the local injection of AAV-FAT10 and AAV-Control in bilateral gonadal white adipose tissue (gWAT) (Biorender). (B) Pairwise comparison validating the overexpression of FAT10. (C)

Hematoxylin and eosin (HE) staining of the locally injected AAV-FAT10 and AAV-Control fat depots showing an increase in the number of small adipocytes with FAT10 overexpression. (D) Quantification of cell area and density through *Adiposoft*. Validated an increase in small adipocyte density with upregulated FAT10.

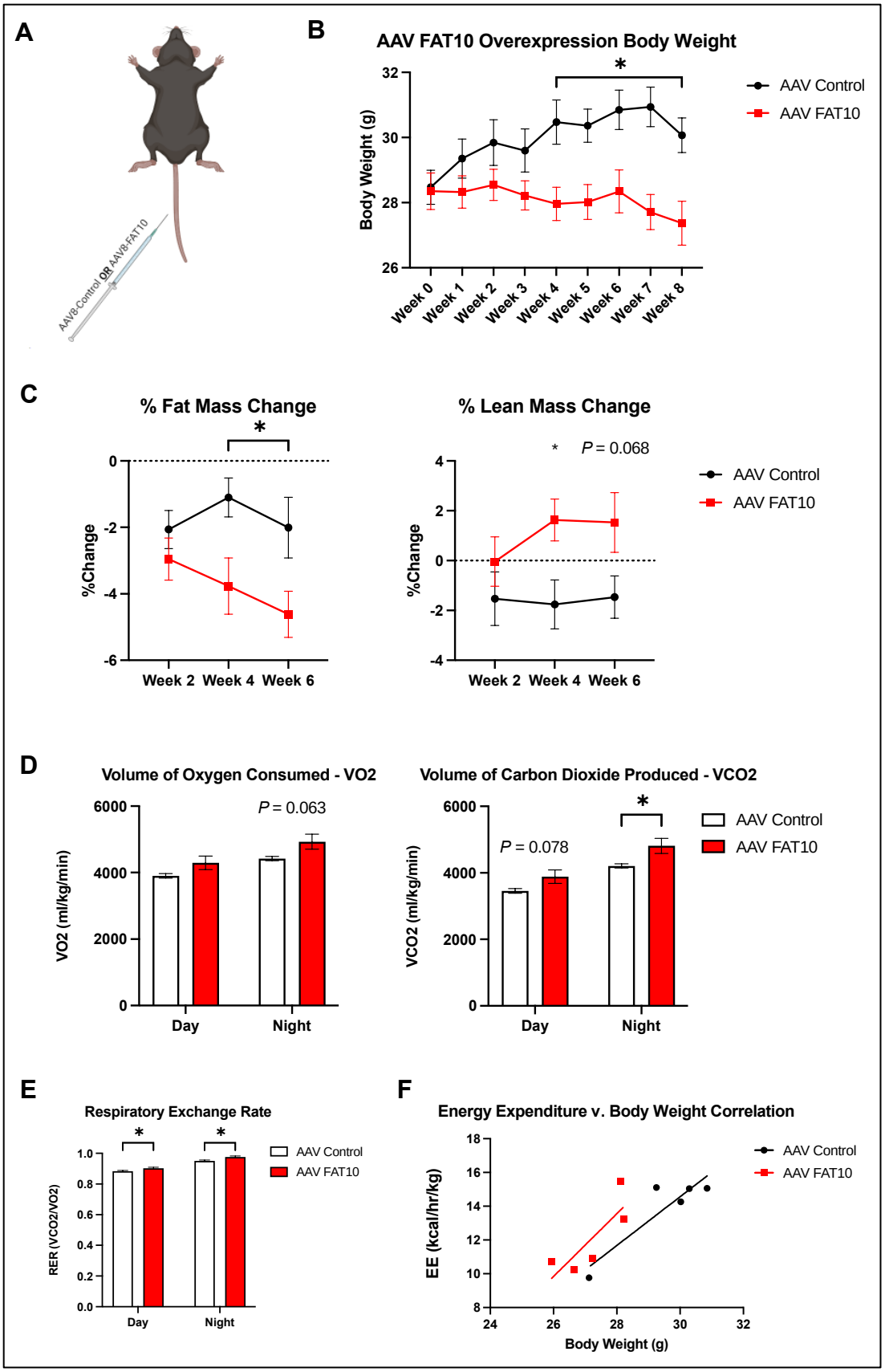
A
AAV8-Control OR AAV8-FAT10
B
AAV FAT10 Overexpression Body Weight
Body Weight (g)
32
30
28
26
*
Week 0
Week 1
Week 2
Week 3
Week 4
Week 5
Week 6
Week 7
Week 8
AAV Control
AAV FAT10
C
% Fat Mass Change
%Change
0
-2
-4
-6
*
Week 2
Week 4
Week 6
% Lean Mass Change
* P = 0.068
4
2
0
-2
-4
AAV Control
AAV FAT10
D
Volume of Oxygen Consumed - VO2
VO2 (ml/kg/min)
6000
4000
2000
0
P = 0.063
Day
Night
Volume of Carbon Dioxide Produced - VCO2
VCO2 (ml/kg/min)
P = 0.078
*
AAV Control
AAV FAT10
E
Respiratory Exchange Rate
RER (VCO2/VO2)
1.0
0.8
0.6
0.4
0.2
0.0
*
*
Day
Night
AAV Control
AAV FAT10
F
Energy Expenditure v. Body Weight Correlation
EE (kcal/hr/kg)
18
16
14
12
10
8
24
26
28
30
32
Body Weight (g)
AAV Control
AAV FAT10

Figure 3. Adipose-specific FAT10 overexpression affects energy homeostasis and metabolism. (A) Schematic depicting the injection of AAV-FAT10 or AAV-Control through the lateral tail vein (Biorender). (B) Body weight measurements across 8-weeks showing significant mitigated weight gain starting at week 4 with AAV-FAT10 mice. (C) Body composition measurements showing AAV-FAT10 mice decreasing in fat mass and increasing in lean mass across time. (D) Respirometry data showing increase of volume of oxygen consumed and carbon dioxide produced in AAV-FAT10 mice. (E) Respiratory exchange rate is increased with AAV-FAT10 mice. (F) Energy expenditure correlated with body weight shows increase trends with FAT10 overexpression. Data are presented as mean ± SEM. * $p < 0.05$, ** $p < 0.005$.

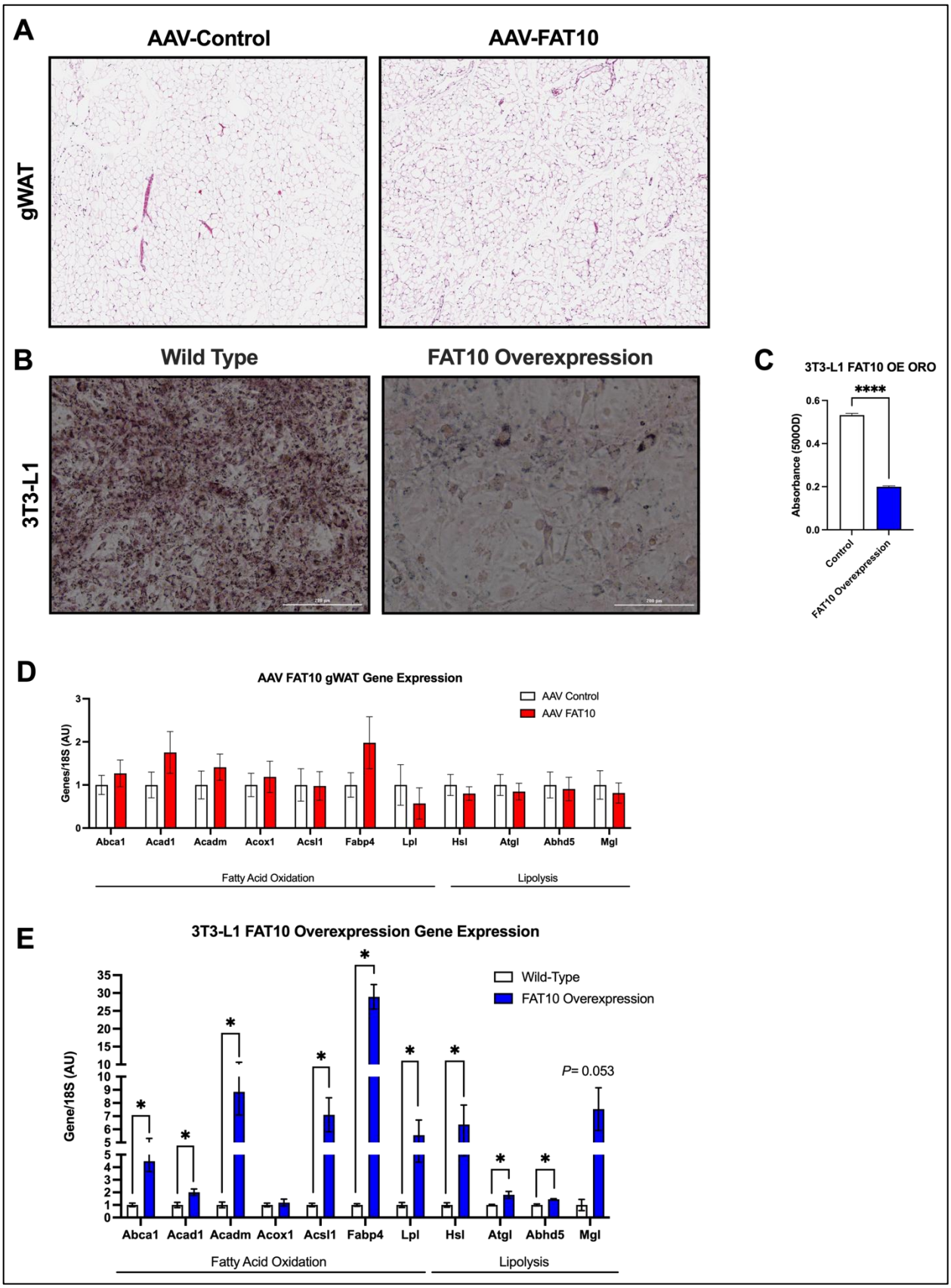
A
AAV-Control
AAV-FAT10
gWAT
B
Wild Type
FAT10 Overexpression
3T3-L1
C
3T3-L1 FAT10 OE ORO
****
Absorbance (500OD)
0.6
0.4
0.2
0.0
Control
FAT10 Overexpression
D
AAV FAT10 gWAT Gene Expression
AAV Control
AAV FAT10
Genes/18S (AU)
3
2
1
0
Abca1
Acad1
Acadm
Acox1
Acsl1
Fabp4
Lpl
Hsl
Atgl
Abhd5
Mgl
Fatty Acid Oxidation
Lipolysis
E
3T3-L1 FAT10 Overexpression Gene Expression
Wild-Type
FAT10 Overexpression
Gene/18S (AU)
35
30
25
20
15
10
10
9
8
7
6
5
5
4
3
2
1
0
P= 0.053
Abca1
Acad1
Acadm
Acox1
Acsl1
Fabp4
Lpl
Hsl
Atgl
Abhd5
Mgl
Fatty Acid Oxidation
Lipolysis

Figure 4. FAT10 regulates lipids metabolism through lipolysis and fatty acid oxidation. (A) HE shows an increased number of smaller adipocytes in the gWAT of AAV-FAT10 mice compared to controls. (B) Oil Red O (ORO) staining in 3T3-L1 differentiated adipocytes with a significant decrease in lipid droplets indicated by red staining with FAT10 overexpression. (C) Optical density (OD) quantification at an absorbance 500 nanometers (nm) showing a significant decrease in ORO staining with FAT10 overexpression. (D) Gene expression in gWAT of AAV-FAT10 mice showing a trending upregulation of fatty acid oxidation and lipolysis related genes. (E) Gene expression in 3T3-L1 differentiated adipocytes showing a statistically significant increase in fatty acid oxidation and lipolysis. Data are presented as mean ± SEM. * $p < 0.05$, ** $p < 0.005$, *** $p < 0.0005$, **** $p < 0.00005$.

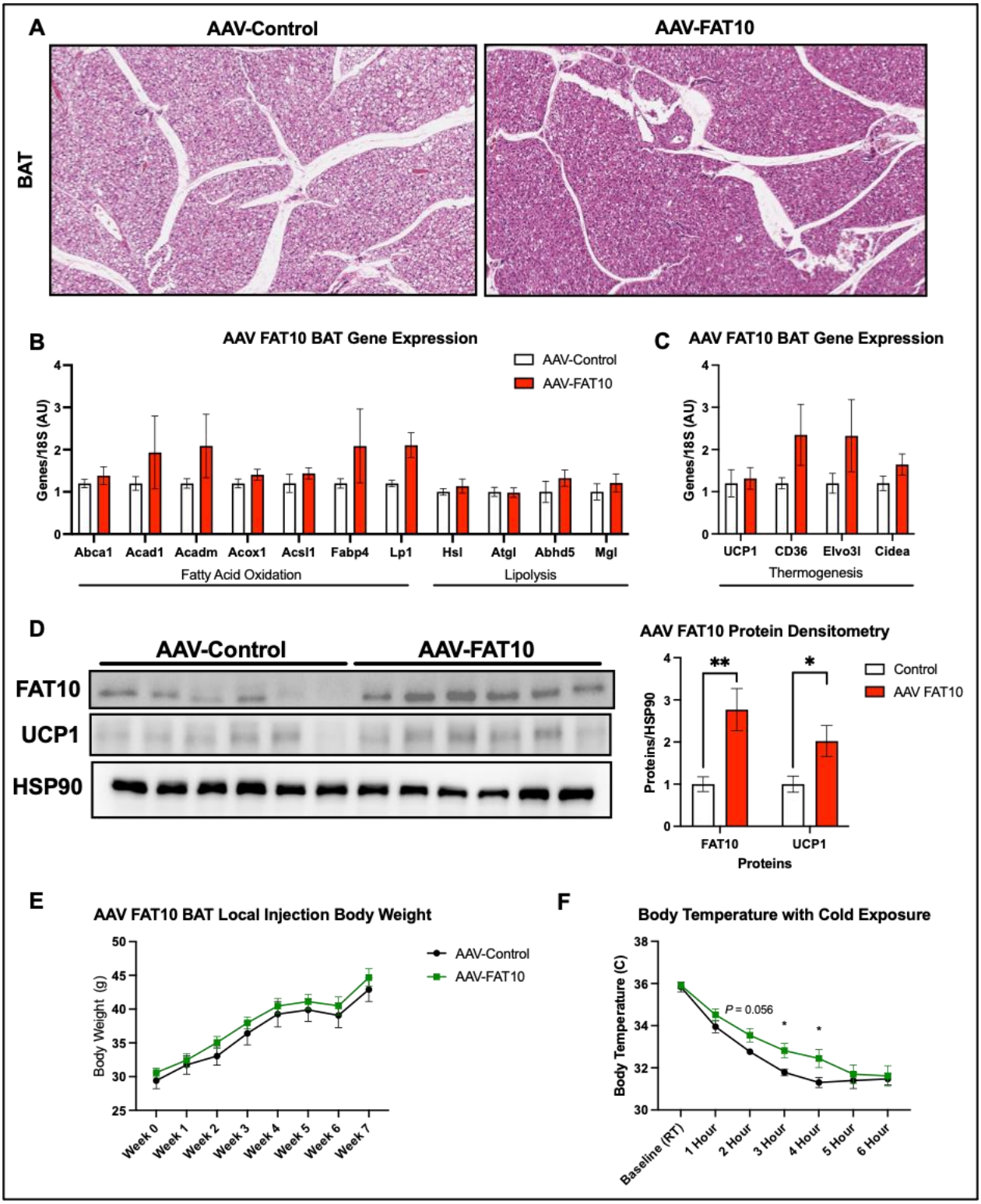

Figure 5. FAT10 regulates UCP1-dependent thermogenesis. (A) HE of brown adipose tissue (BAT) between AAV-Control and AAV-FAT10 mice. (B) Gene expression in BAT for genes

related to fatty acid oxidation and lipolysis trending upwards. (C) Gene expression in BAT for UCP1 show no significant trends or differences. Other thermogenesis-related genes trending upwards. (D) Immunoblot and protein densitometry analysis of FAT10 and UCP1 protein levels, where both are significantly increased. (E) Body weight of BAT-AAV-FAT10 mice across 7 weeks with no change. (F) Baseline body temperature at room temperature (21°C) following six hours of cold exposure (4°C). BAT-AAV-FAT10 mice are capable of maintaining body temperature up to four hours of cold exposure compared to controls. Data are presented as mean ± SEM. * $p < 0.05$, ** $p < 0.005$.

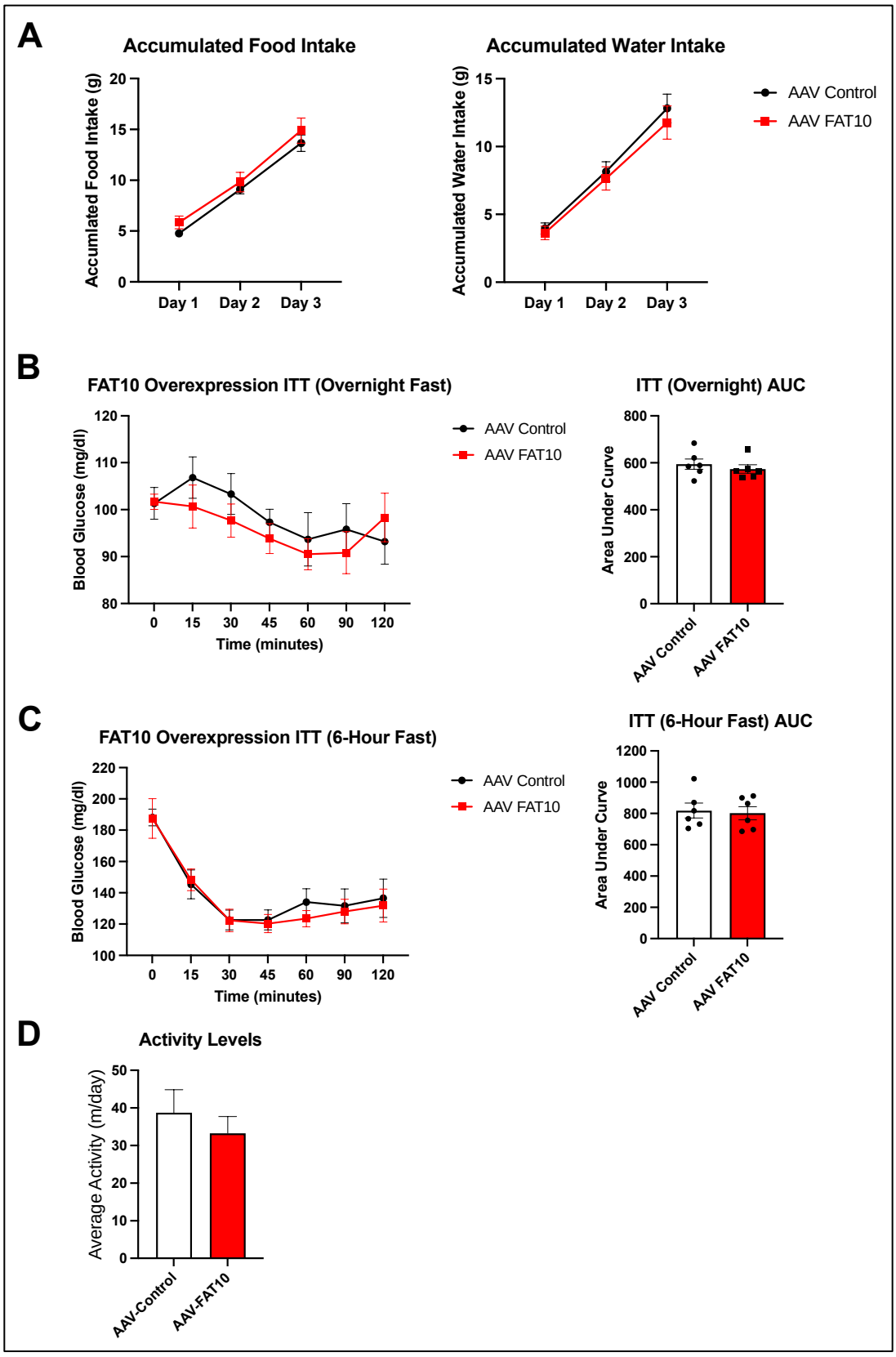
A
Accumulated Food Intake
Accumulated Food Intake (g)
20
15
10
5
0
Day 1
Day 2
Day 3
Accumulated Water Intake
Accumulated Water Intake (g)
15
10
5
0
Day 1
Day 2
Day 3
AAV Control
AAV FAT10
B
FAT10 Overexpression ITT (Overnight Fast)
Blood Glucose (mg/dl)
120
110
100
90
80
0
15
30
45
60
90
120
Time (minutes)
AAV Control
AAV FAT10
ITT (Overnight) AUC
Area Under Curve
800
600
400
200
0
AAV Control
AAV FAT10
C
FAT10 Overexpression ITT (6-Hour Fast)
Blood Glucose (mg/dl)
220
200
180
160
140
120
100
0
15
30
45
60
90
120
Time (minutes)
AAV Control
AAV FAT10
ITT (6-Hour Fast) AUC
Area Under Curve
1200
1000
800
600
400
200
0
AAV Control
AAV FAT10
D
Activity Levels
Average Activity (m/day)
50
40
30
20
10
0
AAV-Control
AAV-FAT10

Supplemental Figure 1. (A) Measurements of accumulated food and water intake across three days showing no significant differences. (B) Intraperitoneal insulin tolerance test (ITT) with an overnight (16-hour) fast showing no significant difference between cohorts. (C) Intraperitoneal ITT with a 6-hour fast showing no significant difference between cohorts. (D) Average activity levels in meters (m) per day measured across three days in the metabolic chamber have no significant difference.

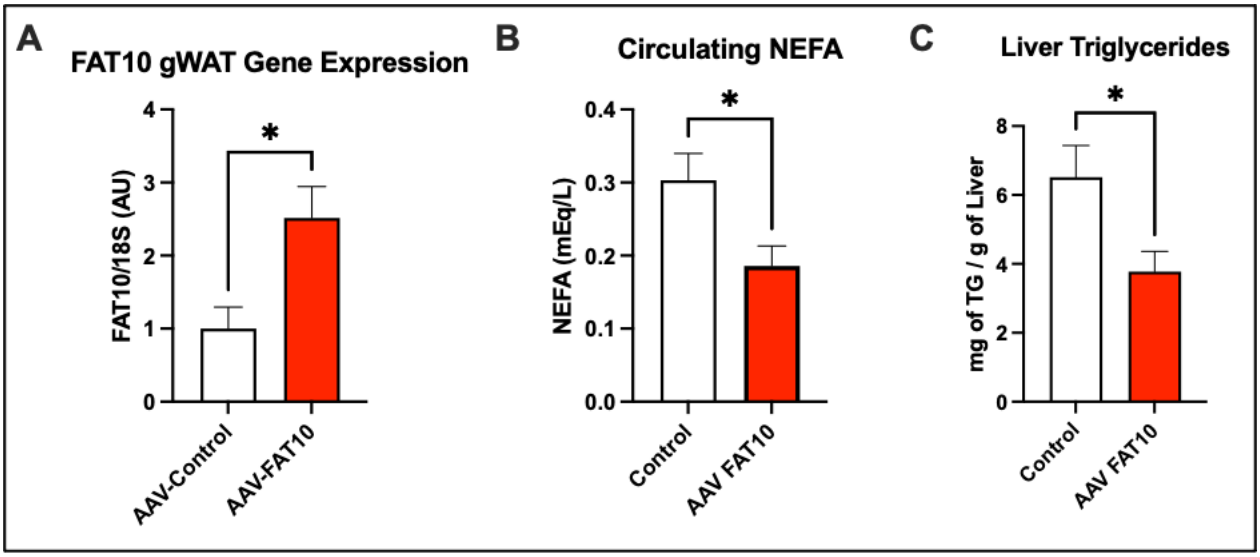

Supplemental Figure 2. (A) FAT10 gene expression in gonadal white adipose tissue between AAV-Control and AAV-FAT10 mice. (B) Non-esterified fatty acids (NEFA) measured in circulating plasma showing a significant decreased in AAV-FAT10 mice. (C) Liver triglycerides (TG) significantly decreased in AAV-FAT10 mice. Data are presented as mean ± SEM. * $p < 0.05$, ** $p < 0.005$.

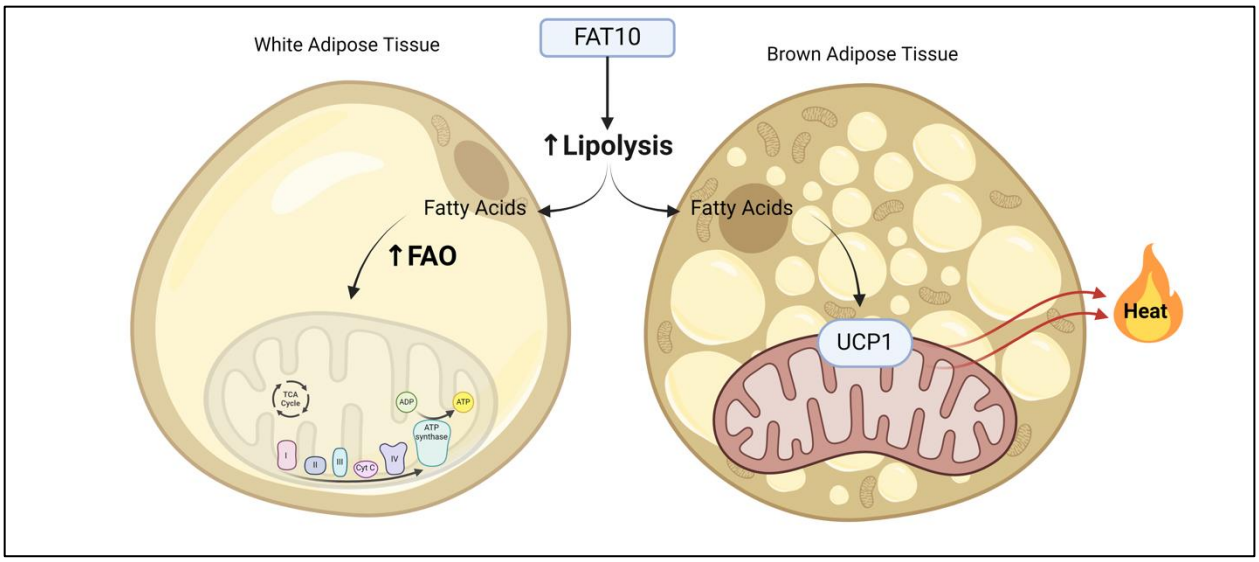

Graphical Abstract. FAT10 plays an important role in the breakdown of triglycerides and lipids in both white and brown adipose tissue through lipolysis. Fatty acids from these processes are then used to fuel catabolic processes such as fatty acid oxidation (FAO) and UCP1-dependent thermogenesis, influencing energy homeostasis.

Discussion

In this study, we provided evidence that ubiquitin-like modifier FAT10 plays a critical role in regulating lipid metabolism in white and brown adipose tissue. Beyond its high inducibility to inflammatory ligands and its downstream effects in immune-related pathologies, FAT10 facilitates the breakdown of lipid stores in adipose tissue to fuel catabolic processes such as fatty acid oxidation and UCP1-dependent thermogenesis.

Present literature has extensively described the mechanism of action of FAT10 in neurodegenerative diseases and cancer[6,8,11,12,14]. However, there continues to be a lack of consensus of how perturbations of FAT10 are associated with various pathologies. A study looking at the global knockout of FAT10 saw modulations in adiposity through upregulation of beta-oxidation in skeletal muscle and increases in energy expenditure[3]. While fatty acid oxidation and energy expenditure is upregulated in our adipose-specific overexpression model, the phenotypes present in the global knockout may be due to a compensatory response or complex organ crosstalk due to the ubiquitous loss of FAT10. Another study utilizing a tissue-specific overexpression of FAT10 in the liver showed impairments of peroxisome proliferator-activated receptor α (PPARα)-mediated lipid metabolism and accumulation of lipids resembling phenotypes of metabolic-dysfunction associated steatotic liver disease (MASLD)[28]. Herein, our study sought to investigate the role of FAT10 in adipose tissue to contribute to a better understanding of its role in a tissue-specific manner.

Through our studies, we provide evidence of how expression of FAT10 variable and dynamic given different conditions of adipose physiology. With chronic, voluntary exercise, mice exhibit an overall decrease in adipose FAT10 expression that parallels decrease in adiposity. However, with varying timepoints of post-exercise recovery after acute treadmill

running, we find that adipose FAT10 is variable with dynamic protein levels. To investigate the adipose-specific role of FAT10, we first constructed an adiponectin-driven AAV that was locally injected to the gWAT. Herein, we saw significant changes in adipose morphology, where the white adipose depot presented with an increase number of small adipocytes compared to its internal control. To investigate the effects on adipose metabolism, AAV-FAT10 was administrated through the tail vein which result in mitigated weight gain and a significant decrease in fat mass. Further studies then demonstrated an overall increase in lipolysis, decreasing the lipid droplets stored in both white and brown adipose tissue. Interestingly, energy expenditure was also increased with adipose FAT10 expression levels, leading us to identify an increase in catabolic processes such as fatty acid oxidation and non-shivering UCP1-mediated thermogenesis. While our findings begin to characterize the role of FAT10 in white and brown adipose tissue, further experimentation describing FAT10 as a ubiquitin-like modifier and its role in regulating protein stabilization and localization may improve our understanding of its mechanistic regulation of metabolic processes.

Together, we show the dynamic expression of FAT10 in adipose tissue and how it regulates energy homeostasis by breaking down lipid stores through lipolysis to fuel energy-demanding metabolic pathways like fatty acid oxidation and thermogenesis (Graphical Abstract). More importantly, our study emphasizes the importance of studying FAT10 in a tissue-specific manner to further improve our understanding of the role of FAT10 in metabolism. These findings suggest that FAT10 is essential in the homeostatic regulation of energy metabolism, suggesting that FAT10 may be a target for future therapeutic interventions for obesity and metabolically associated diseases.

Conclusion

Our findings suggest that FAT10 plays a pivotal role in regulating lipolysis pathways in both white and brown adipose tissue, where lipid stores are broken down into fatty acids to fuel catabolic and energetic pathways. Primarily, these catabolic pathways consist of an upregulation of fatty acid oxidation and UCP1-dependent thermogenesis. This study also emphasizes the importance of studying FAT10 in a tissue-specific manner to better characterize its role in the scheme of whole-body physiology and metabolism. Together, this study suggests that FAT10 may be targeted as a therapeutic to potentially ameliorate the burden of obesity and metabolically associated disease.

References

1. Groettrup, M., et al. Activating the ubiquitin family: UBA6 challenges the field. *Trends Biochem. Sci.* 33, 230–237 (2008).
2. Deng, X., et al. Ubiquitin-like protein FAT10 promotes osteosarcoma glycolysis and growth by upregulating PFKFB3 via stabilization of EGFR. *Am J Cancer*. 2020 Jul 1;10(7):2066-2082.
3. Canaan, D.J., et al. Extended lifespan and reduced adiposity in mice lacking the FAT10 gene. *PNAS*. (2014), 5313-8, 111(14).
4. Wimalarathne, M., et al. The case for FAT10 as a novel target in fatty liver diseases. *Frontiers in Pharmacology*. (2022), 972320, 13.
5. Aichem, A., et al. The ubiquitin-like modifier FAT10 - much more than a proteasome-targeting signal. *Journal of Cell Science*. (2020), 133(14).
6. Schregle, R., et al. The expression profile of the ubiquitin-like modifier FAT10 in immune cells suggests cell type-specific functions. *Immunogenetics*. (2018), 429-438, 70(7).
7. Aichem A, Kalveram B, Spinnenhirn V, Kluge K, Catone N, Johansen T, Groettrup M. The proteomic analysis of endogenous FAT10 substrates identifies p62/SQSTM1 as a substrate of FAT10ylation. J Cell Sci. 2012 Oct 1;125(Pt 19):4576-85. doi: 10.1242/jcs.107789. Epub 2012 Jul 13. PMID: 22797925.
8. Zhu J, Zhao J, Luo C, Zhu Z, Peng X, Zhu X, Lin K, Bu F, Zhang W, Li Q, Wang K, Hu Z, Yu X, Chen L, Yuan R. FAT10 promotes chemotherapeutic resistance in pancreatic cancer by inducing epithelial-mesenchymal transition via stabilization of FOXM1

expression. Cell Death Dis. 2022 May 25;13(5):497. doi: 10.1038/s41419-022-04960-0. PMID: 35614040; PMCID: PMC9132907.

9. Liu, X., Ge, J., Chen, C. et al. FAT10 protects against ischemia-induced ventricular arrhythmia by decreasing Nedd4-2/Nav1.5 complex formation. Cell Death Dis 12, 25 (2021). https://doi.org/10.1038/s41419-020-03290-3
10. Hipp MS, Kalveram B, Raasi S, Groettrup M, Schmidtke G. FAT10, a ubiquitin-independent signal for proteasomal degradation. Mol Cell Biol. 2005 May;25(9):3483-91. doi: 10.1128/MCB.25.9.3483-3491.2005. PMID: 15831455; PMCID: PMC1084302.
11. Cerqueira É, Marinho DA, Neiva HP, Lourenço O. Inflammatory Effects of High and Moderate Intensity Exercise-A Systematic Review. Front Physiol. 2020 Jan 9;10:1550. doi: 10.3389/fphys.2019.01550. PMID: 31992987; PMCID: PMC6962351.
12. Roverato ND, Sailer C, Catone N, Aichem A, Stengel F, Groettrup M. Parkin is an E3 ligase for the ubiquitin-like modifier FAT10, which inhibits Parkin activation and mitophagy. Cell Rep. 2021 Mar 16;34(11):108857. doi: 10.1016/j.celrep.2021.108857. PMID: 33730565.
13. Moore TM, Cheng L, Wolf DM, Ngo J, Segawa M, Zhu X, Strumwasser AR, Cao Y, Clifford BL, Ma A, Scumpia P, Shirihai OS, Vallim TQA, Laakso M, Lusis AJ, Hevener AL, Zhou Z. Parkin regulates adiposity by coordinating mitophagy with mitochondrial biogenesis in white adipocytes. Nat Commun. 2022 Nov 4;13(1):6661. doi: 10.1038/s41467-022-34468-2. PMID: 36333379; PMCID: PMC9636263.
14. Yuan R, Wang K, Hu J, Yan C, Li M, Yu X, Liu X, Lei J, Guo W, Wu L, Hong K, Shao J. Ubiquitin-like protein FAT10 promotes the invasion and metastasis of hepatocellular

carcinoma by modifying β-catenin degradation. Cancer Res. 2014 Sep 15;74(18):5287-300. doi: 10.1158/0008-5472.CAN-14-0284. Epub 2014 Jul 23. PMID: 25056121.

15. Ikeda K, Yamada T. UCP1 Dependent and Independent Thermogenesis in Brown and Beige Adipocytes. Front Endocrinol (Lausanne). 2020 Jul 28;11:498. doi: 10.3389/fendo.2020.00498. PMID: 32849287; PMCID: PMC7399049.
16. Crichton PG, Lee Y, Kunji ER. The molecular features of uncoupling protein 1 support a conventional mitochondrial carrier-like mechanism. Biochimie. 2017 Mar;134:35-50. doi: 10.1016/j.biochi.2016.12.016. Epub 2017 Jan 3. PMID: 28057583; PMCID: PMC5395090.
17. Vangipurapu J, Stančáková A, Pihlajamäki J, Kuulasmaa TM, Kuulasmaa T, Paananen J, Kuusisto J, Ferrannini E, Laakso M. Association of indices of liver and adipocyte insulin resistance with 19 confirmed susceptibility loci for type 2 diabetes in 6,733 non-diabetic Finnish men. Diabetologia. 2011 Mar;54(3):563-71. doi: 10.1007/s00125-010-1977-4. Epub 2010 Dec 12. PMID: 21153532.
18. Moore TM, Lee S, Olsen T, Morselli M, Strumwasser AR, Lin AJ, Zhou Z, Abrishami A, Garcia SM, Bribiesca J, Cory K, Whitney K, Ho T, Ho T, Lee JL, Rucker DH, Nguyen CQA, Anand ATS, Yackly A, Mendoza LQ, Leyva BK, Aliman C, Artiga DJ, Meng Y, Charugundla S, Pan C, Jedian V, Seldin MM, Ahn IS, Diamante G, Blencowe M, Yang X, Mouisel E, Pellegrini M, Turcotte LP, Birkeland KI, Norheim F, Drevon CA, Lusis AJ, Hevener AL. Conserved multi-tissue transcriptomic adaptations to exercise training in humans and mice. Cell Rep. 2023 May 30;42(5):112499. doi: 10.1016/j.celrep.2023.112499. Epub 2023 May 12. PMID: 37178122.

19. Zhou M, Tamburini IJ, Van C, Molendijk J, Nguyen CM, Chang IY, Johnson C, Velez LM, Cheon Y, Yeo RX, Bae H, Le J, Larson N, Pulido R, Filho C, Jang C, Marazzi I, Justice JN, Pannunzio N, Hevener A, Sparks LM, Kershaw EE, Nicholas D, Parker B, Masri S, Seldin M. Leveraging inter-individual transcriptional correlation structure to infer discrete signaling mechanisms across metabolic tissues. bioRxiv [Preprint]. 2023 Oct 4:2023.05.10.540142. doi: 10.1101/2023.05.10.540142. Update in: This article has been published with doi: 10.7554/eLife.88863.3. Update in: Elife. 2024 Jan 15;12: PMID: 37214953; PMCID: PMC10197628.
20. Seldin MM, Koplev S, Rajbhandari P, Vergnes L, Rosenberg GM, Meng Y, Pan C, Phuong TMN, Gharakhanian R, Che N, Mäkinen S, Shih DM, Civelek M, Parks BW, Kim ED, Norheim F, Chella Krishnan K, Hasin-Brumshtein Y, Mehrabian M, Laakso M, Drevon CA, Koistinen HA, Tontonoz P, Reue K, Cantor RM, Björkegren JLM, Lusis AJ. A Strategy for Discovery of Endocrine Interactions with Application to Whole-Body Metabolism. Cell Metab. 2018 May 1;27(5):1138-1155.e6. doi: 10.1016/j.cmet.2018.03.015. PMID: 29719227; PMCID: PMC5935137.
21. Galarraga M, Campión J, Muñoz-Barrutia A, Boqué N, Moreno H, Martínez JA, Milagro F, Ortiz-de-Solórzano C. Adiposoft: automated software for the analysis of white adipose tissue cellularity in histological sections. J Lipid Res. 2012 Dec;53(12):2791-6. doi: 10.1194/jlr.D023788. Epub 2012 Sep 19. Erratum in: J Lipid Res. 2014 Dec;55(12):2705. PMID: 22993232; PMCID: PMC3494244.
22. van der Stelt I, Hoevenaars F, Široká J, de Ronde L, Friedecký D, Keijer J, van Schothorst E. Metabolic Response of Visceral White Adipose Tissue of Obese Mice Exposed for 5 Days to Human Room Temperature Compared to Mouse

Thermoneutrality. Front Physiol. 2017 Mar 23;8:179. doi: 10.3389/fphys.2017.00179. PMID: 28386236; PMCID: PMC5362617.

23. Zhou Mingqi, Tamburini Ian J., Van Cassandra, Molendijk Jeffrey, Nguyen Christy M, Chang Ivan Yao-Yi, Johnson Casey, Velez Leandro M., Cheon Youngseo, Yeo Reichelle X., Bae Hosung, Le Johnny, Larson Natalie, Pulido Ron, Filho Carlos, Jang Cholsoon, Marazzi Ivan, Justice Jamie N., Pannunzio Nicholas, Hevener Andrea, Sparks Lauren M., Kershaw Erin E., Nicholas Dequina, Parker Benjamin, Masri Selma, Seldin Marcus (2023) Leveraging inter-individual transcriptional correlation structure to infer discrete signaling mechanisms across metabolic tissues eLife 12:RP88863. https://doi.org/10.7554/eLife.88863.2
24. Laakso M, Kuusisto J, Stančáková A, Kuulasmaa T, Pajukanta P, Lusis AJ, Collins FS, Mohlke KL, Boehnke M. The Metabolic Syndrome in Men study: a resource for studies of metabolic and cardiovascular diseases. J Lipid Res. 2017 Mar;58(3):481-493. doi: 10.1194/jlr.O072629. Epub 2017 Jan 24. PMID: 28119442; PMCID: PMC5335588.
25. Karpe F, Dickmann JR, Frayn KN. Fatty acids, obesity, and insulin resistance: time for a reevaluation. Diabetes. 2011 Oct;60(10):2441-9. doi: 10.2337/db11-0425. PMID: 21948998; PMCID: PMC3178283.
26. Frayn KN, Summers LK, Fielding BA. Regulation of the plasma non-esterified fatty acid concentration in the postprandial state. Proc Nutr Soc. 1997 Jul;56(2):713-21. doi: 10.1079/pns19970071. PMID: 9264121.
27. Cerqueira É, Marinho DA, Neiva HP, Lourenço O. Inflammatory Effects of High and Moderate Intensity Exercise-A Systematic Review. Front Physiol. 2020 Jan 9;10:1550. doi: 10.3389/fphys.2019.01550. PMID: 31992987; PMCID: PMC6962351.

28. Clavreul L, Bernard L, Cotte AK, Hennuyer N, Bourouh C, Devos C, Helleboid A, Haas JT, Verrijken A, Gheeraert C, Derudas B, Guille L, Chevalier J, Eeckhoute J, Vallez E, Dorchies E, Van Gaal L, Lassailly G, Francque S, Staels B, Paumelle R. The ubiquitin-like modifier FAT10 is induced in MASLD and impairs the lipid-regulatory activity of PPARα. Metabolism. 2024 Feb;151:155720. doi: 10.1016/j.metabol.2023.155720. Epub 2023 Nov 3. PMID: 37926201.